

The Consortium for Enabling Technologies and Innovation

Virtual Summer Meeting for Young Researchers

Atomic Layer deposition for microchannel plate applications

Ashwin Jayaraman, Anil Mane and Jeff Elam

Argonne National Laboratory, 9700 S Cass
Avenue, Lemont, IL USA- 60439

July 7 2020



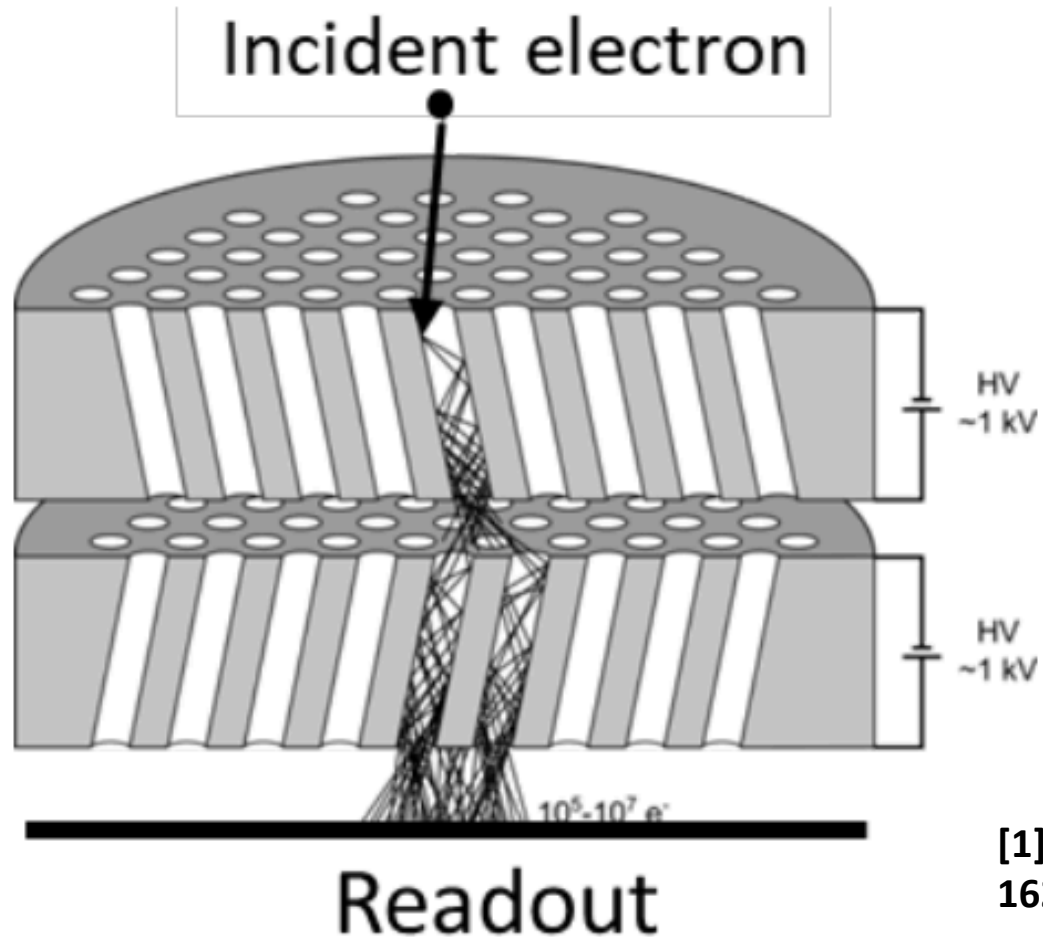
Brief Bio

Jeff Elam is a Senior Chemist and Group Leader at Argonne National Laboratory where he directs a program in atomic layer deposition (ALD) technology

Anil Mane is a Principal Materials Science Engineer at Argonne involved in research and development of next generation photodetectors, 2D materials, functional coatings by ALD/CVD techniques

Ashwin Jayaraman is a Postdoctoral Appointee in Argonne National Laboratory's Applied Materials Division working in Jeff Elam's group.

Microchannel Plates and Operating Principle



MCP – A continuous 2d array of 10^4 to 10^7 micron sized pores, which act as electron amplifiers.

Typical MCPs have a

1. Length over diameter (L/D) ratio of 40:1–80:1
2. Bias angles of 8° - 20°
3. Pore diameters from $10\ \mu\text{m}$ to $40\ \mu\text{m}$, and
4. Open-area ratios ranging from 60% to 83%

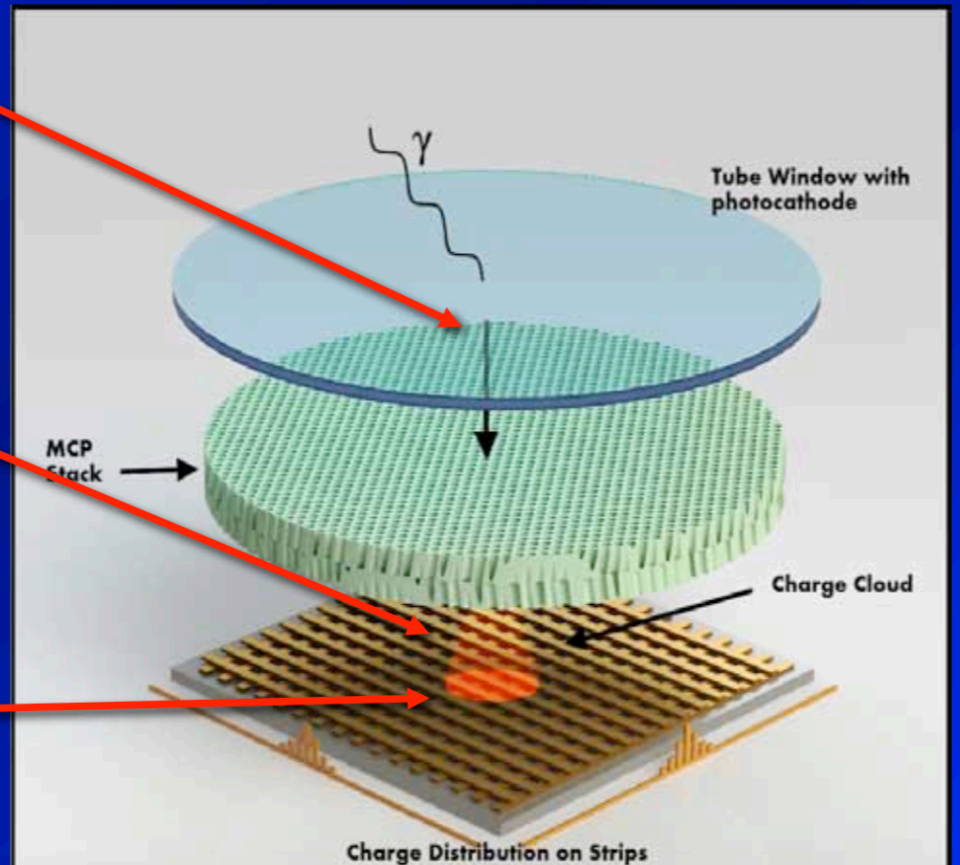
[1] J. L. Wiza, "Microchannel plate detectors," *Nucl. Instrum. Methods*, vol. 162, p. 587, 1979.

Microchannel Plate Photo-detector

Photocathode converts photon to electron

MCP(s) amplify electron by 10^4 to 10^7

Patterned anode measures charge centroid



C. Ertley *et al.*, "Microchannel Plate Imaging Detectors for High Dynamic Range Applications," *IEEE Trans. Nucl. Sci.*, vol. 64, no. 7, pp. 1774–1780, Jul. 2017.

Microchannel Plate Applications

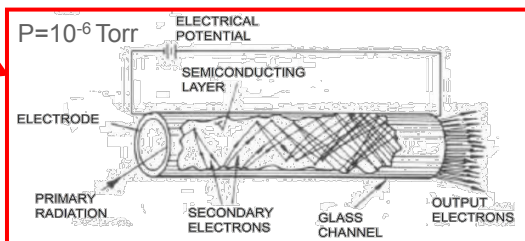
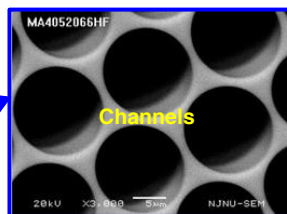
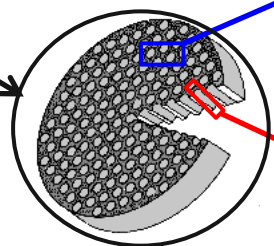
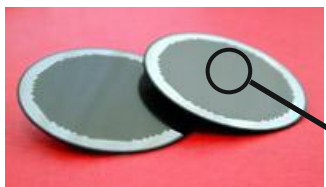
1. Electron spectroscopy and microscopy devices,
2. Photomultiplier tubes (PMTs)
3. Medical imagers
4. Night vision products
5. Cathode ray tubes, image intensifier tubes
6. Time-of-flight (ToF) mass spectrometers
7. Photon counting, imaging microchannel plate sensors are widely used in astronomy, high energy physics and remote sensing
8. Sensing of photons, charged particles, and neutrons accomplished using high detection efficiency photocathodes
9. For space science applications, Large UV/Optical/Infrared Surveyor (LUVOIR) and the Habitable Exoplanet Imaging Mission (HABEX)



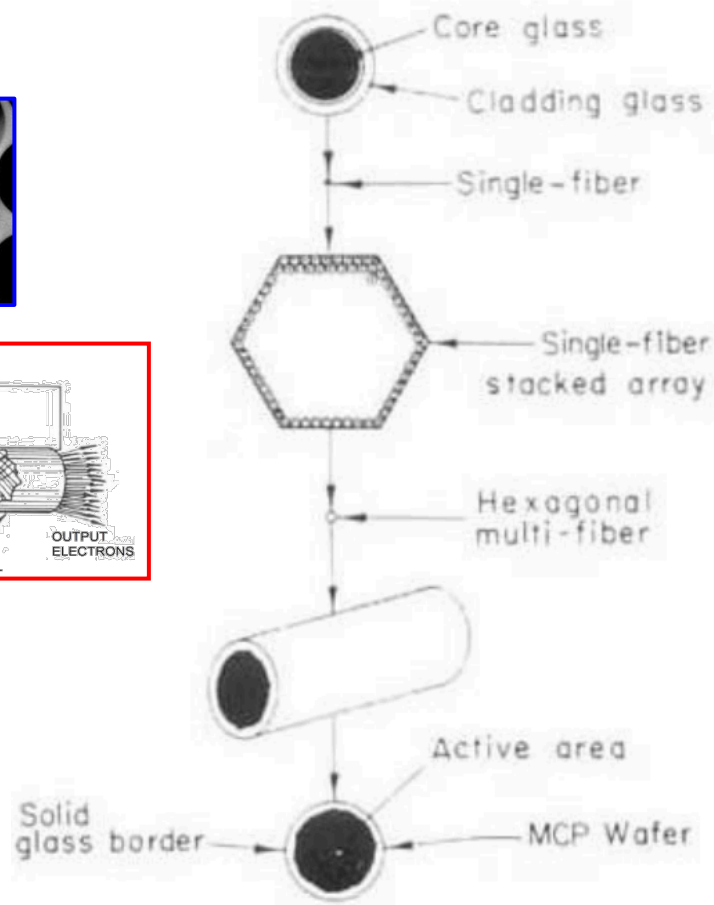
<https://www.azosensors.com/equipment-details>

Conventional Microchannel Plate Fabrication

Conventional MCPs



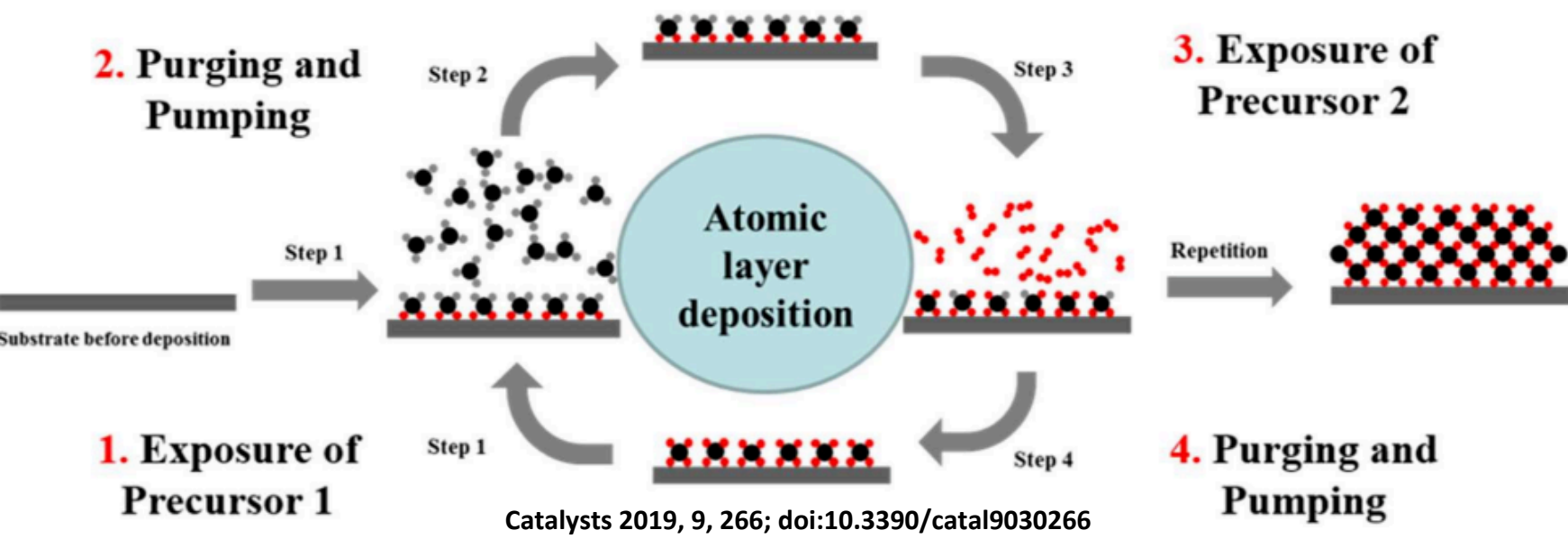
Pore Resistance – $1e12$ to $1e15$ ohm
 MCP Resistance – 10 Mohm – 1Gohm
 ΔV across MCP ≤ 1200 V
 SEE coefficient < 1.5
 Gain – $1e4$ – $1e7$



Conventional MCP Fabrication	
➤ Draw lead glass fiber bundle	
➤ Slice, polish, chemical etch	
➤ Heat in hydrogen	
➤ Top/Bottom electrode coating (NiCr)	
Drawbacks	
➤ Expensive	
➤ MCP resistance and secondary emission properties are linked to semiconducting Pb	
➤ Limited optimize MCP performance for applications where lifetime, gain, substrate size, composition and thermal runaway are important	

[1] J. L. Wiza, "Microchannel plate detectors," *Nucl. Instrum. Methods*, vol. 162, p. 587, 1979

ALD Approach for Large Area Photodetectors (LAPPD) at Argonne



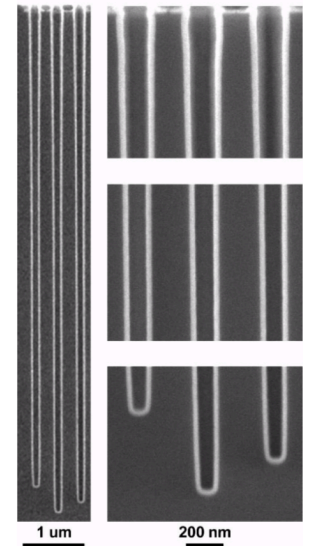
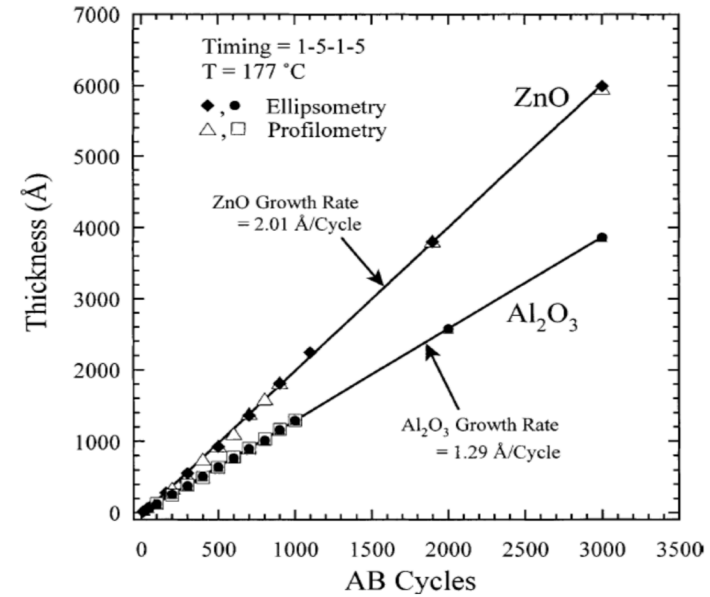
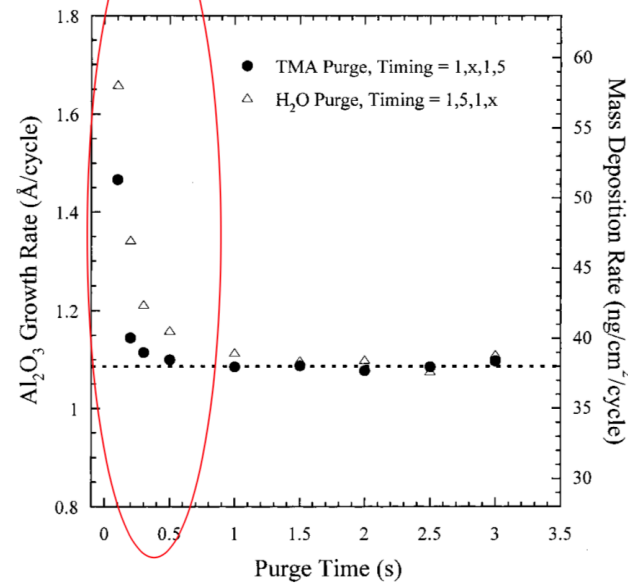
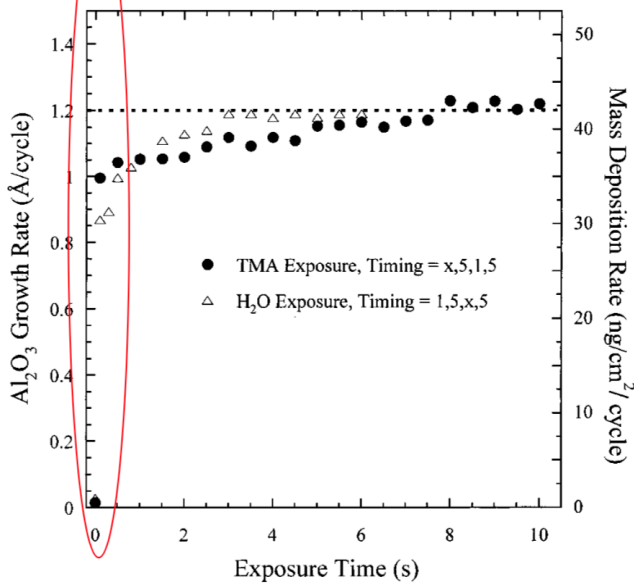
1. Precursor introduced separately in time and space
2. Involves self-limiting film growth via alternate saturated surface reactions
3. Produces wide range of stoichiometric conformal pinhole free films
4. Extremely accurate thickness and composition control of mixed oxides, graded layers
5. Lower deposition temperature can be used for sensitive substrates than in CVD
6. Low impurity level of the films enable excellent physical and chemical properties

Argonne LAPPD Approach
➤ Start with porous, non-lead substrate
➤ ALD (resistive + SEE layer) coating
➤ Thermal treatment
➤ Top/Bottom Electrode coating (NiCr)
Advantages
➤ Independent control over composition of Resistive and SEE coating
➤ Low thermal runaway
➤ Applicable: Ceramics, SiO ₂ , plastics, polymers MCPs
➤ Low cost (No major issue for scale-up with ALD)

**“Made in USA” capabilities
Economical**

Optimization of dose purge parameters and linearity in growth

Quartz crystal Microbalance results



Elam *et al*, Rev. Sci. Instrum., Vol. 73, No. 8, August 2002

Elam *et al*, Chem. Mater., Vol. 15, No. 4, 2003

ALD MCP schematic and cross section showing composition

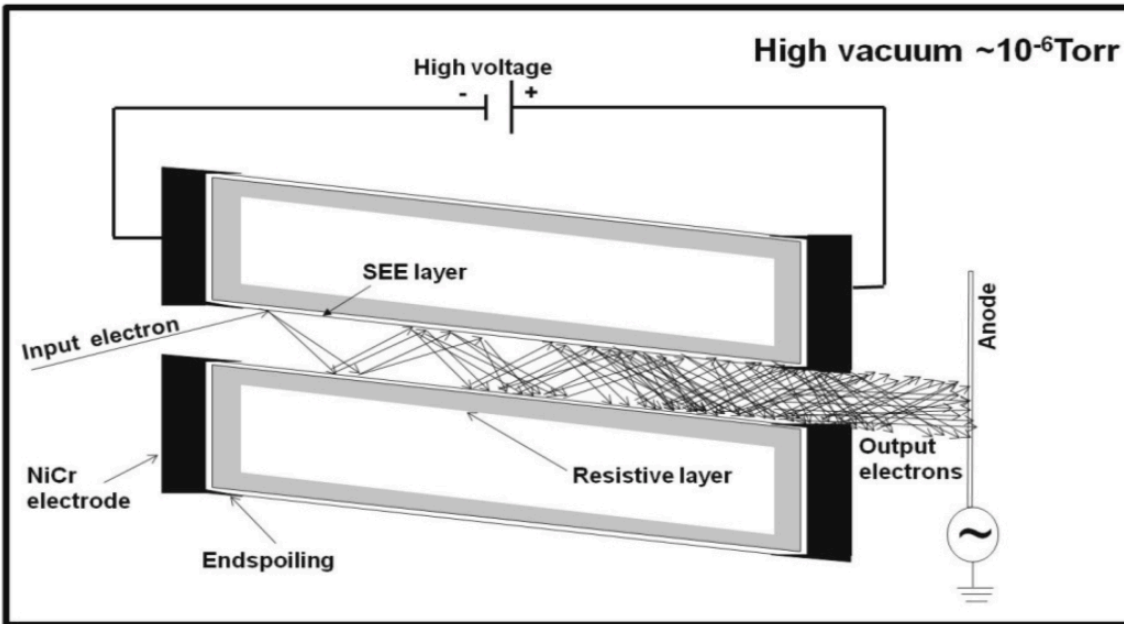
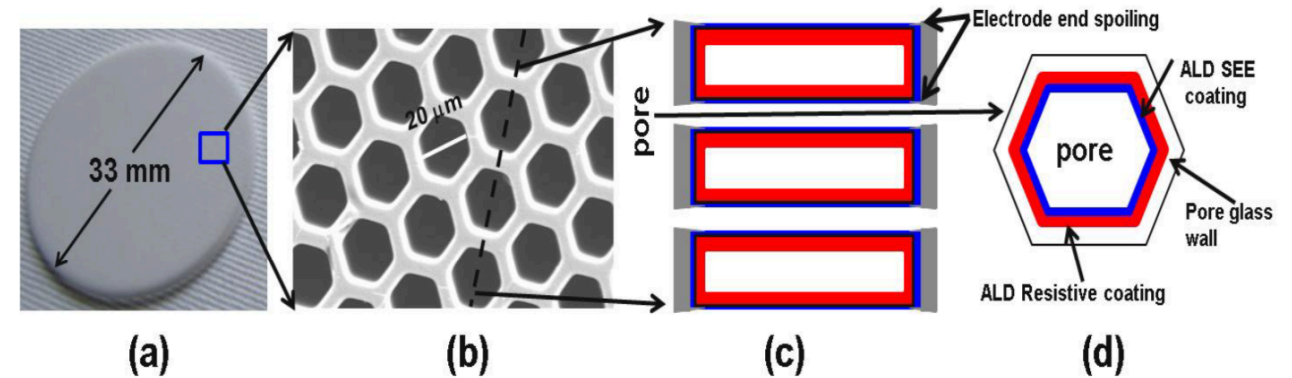


Figure 1. Schematic of basic operation of MCP.



Fabrication sequence of MCP – a) as received capillary glass array substrate, b) plan view SEM of capillary array front surface, c) Schematic cross section of fully functionalized MCP, d) Schematic cross section of individual MCP pore after ALD functionalization

Composed of a) resistive material, b) secondary electron emissive material and c) contact electrodes

A.U. Mane et.al. Physics Procedia 37 (2012) 722 – 732 - An atomic layer deposition method to fabricate economical and robust large area microchannel plates for photodetectors

Material requirements for ALD MCP

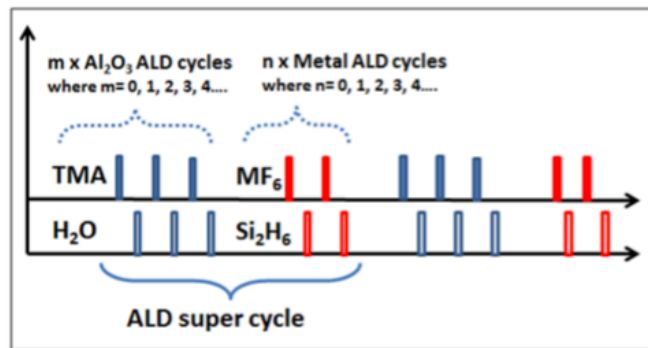
1. Dry and clean porous substrates (Micro-capillary arrays)
2. Uniform and conformal deposition of desire materials by ALD - Stable resistive material layer (to generate electrostatic field)
3. Material resistivity range = $1e6-1e10 \Omega\text{-cm}$
4. Stable secondary electron emission layer (signal amplification)
5. Stable Contact electrode (e.g NiCr, W, TiN, etc.) for electrical contact) especially by PVD electrode penetration normally a pore diameter)

ALD Chemistries for Resistive Coatings

ALD of M-Al₂O₃ Composite Films

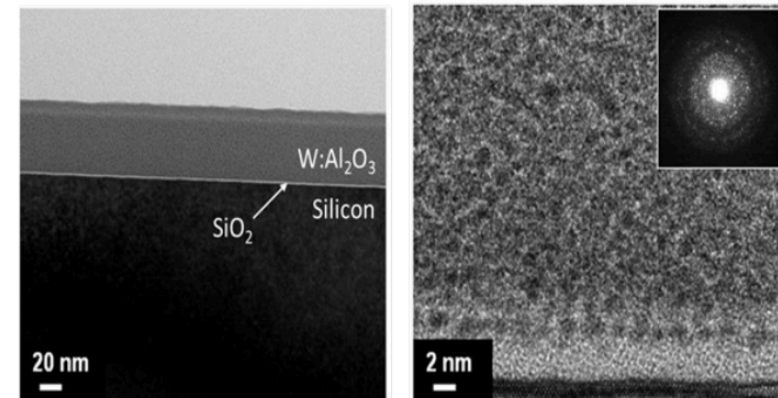
- Combine 2 ALD processes:

- Oxide -- TMA/H₂O → Al₂O₃ : insulator, $\rho=10^{16}$ Ω cm
- Metal -- MF₆/Si₂H₆ → M=W, Mo : conductor, $\rho=10^{-4}$ Ω cm



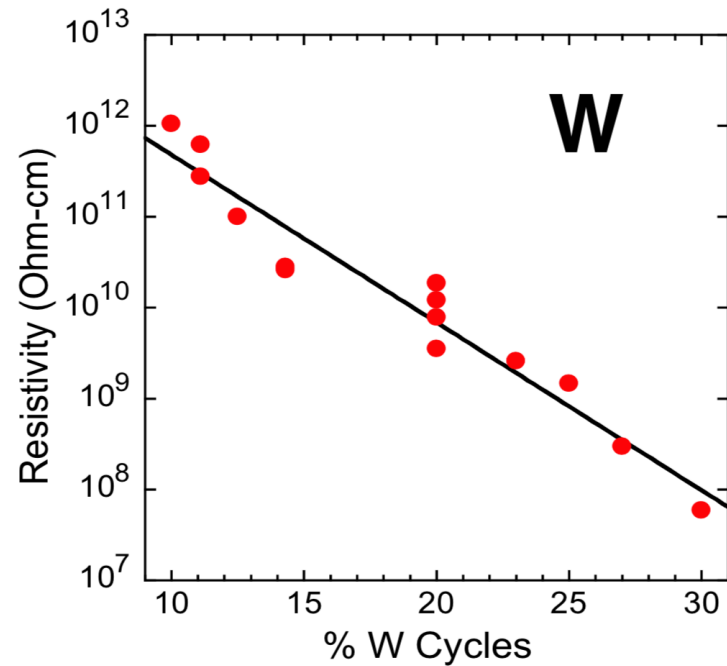
- Adjust resistivity with $M/(M+Al_2O_3)$ cycle ratio
- Deposition Temperature
- Precursors types

- Mid range resistivity targeted – 1e6 to 1e10 ohmcm
- Thin film Material engineered by ALD
- Previous Materials - AlZnOx, NiAlOx, CuAlOx, TaZrOx etc
- Issues: Resistivity control, Stability, Precursors nature, cost
- Current method affords tunable resistance with compatible growth of mixed layers in high aspect ratio structures

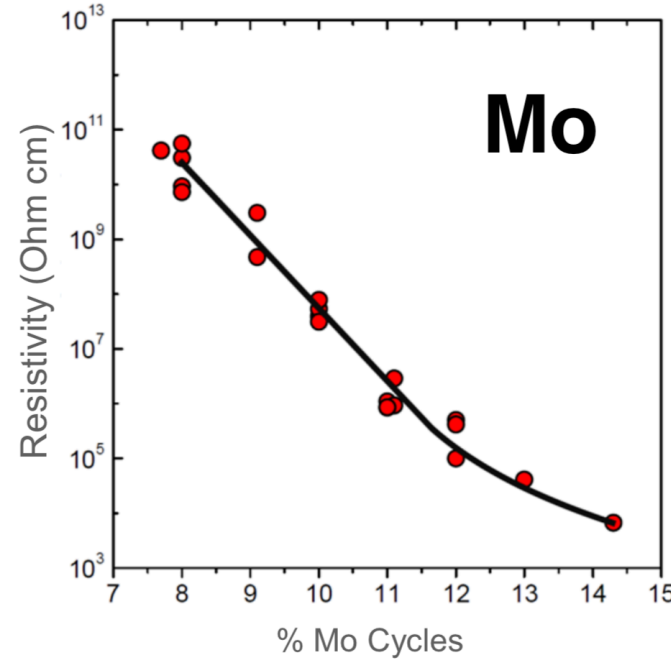


Cross section TEM image of W:Al₂O₃ composite
Mane et al. – Proc SPIE 2013, Cremer et al. – Proc SPIE 2019

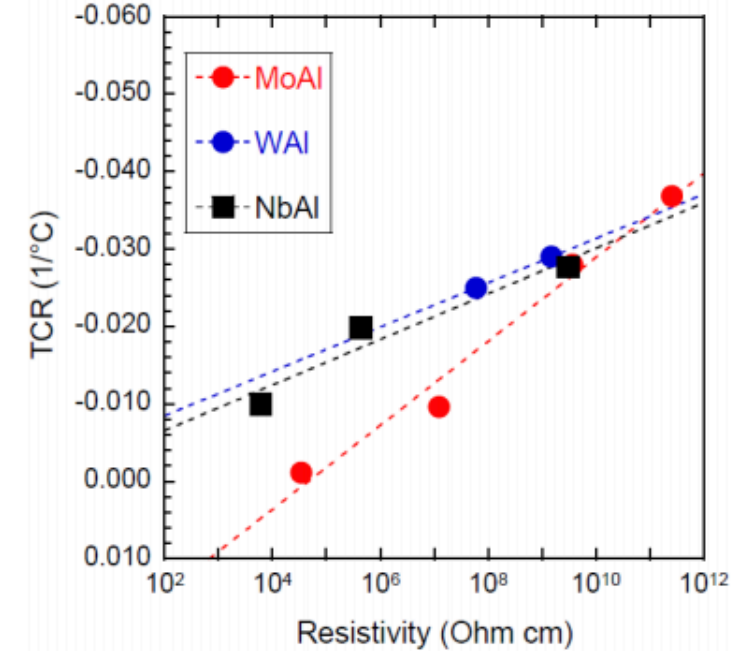
Resistive Materials for MCP - Properties



WAlFOC resistive material resistivity as a function of metal content



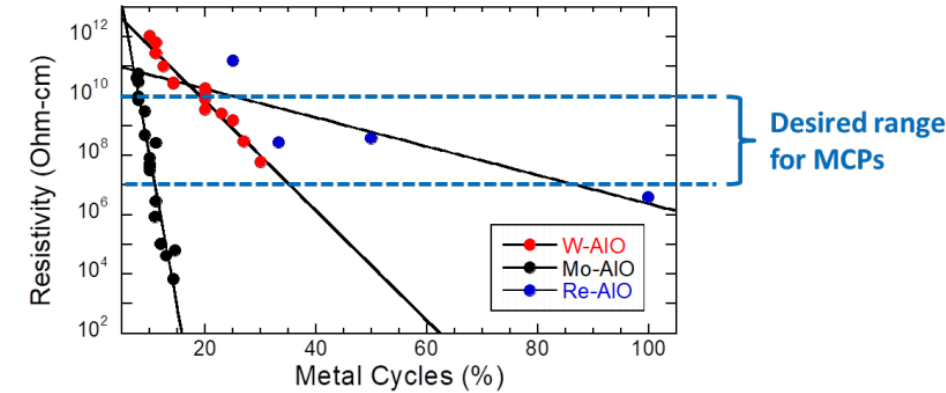
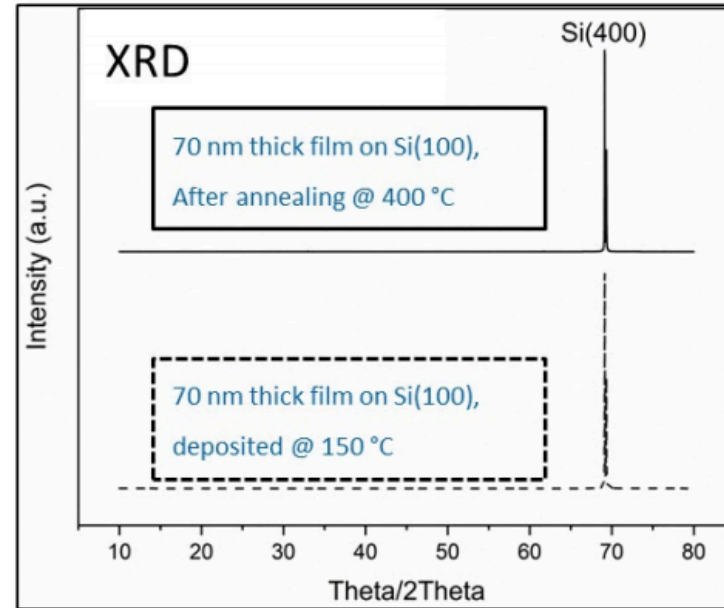
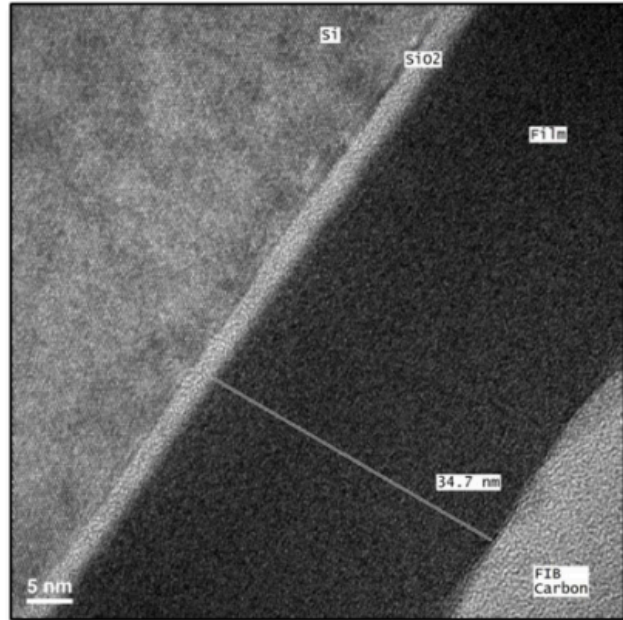
Mo:Al₂O₃ resistive material resistivity as a function of metal content



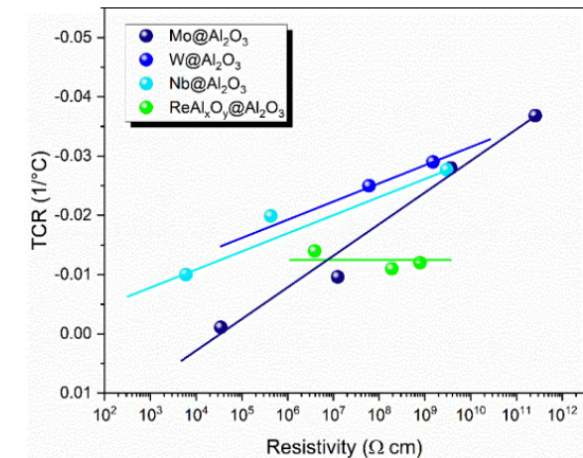
TCR values versus resistivity for M:Al₂O₃ tunable resistance coatings where M=Mo, W and Nb

Mane et al. – Proc SPIE 2013, Cremer et al. – Proc SPIE 2019

Alternative resistive material : $\text{ReAl}_2\text{O}_3\text{CH}_3$



Resistivity as a function of metal cycles - ALD $\text{ReAl}_2\text{O}_3\text{CH}_3$

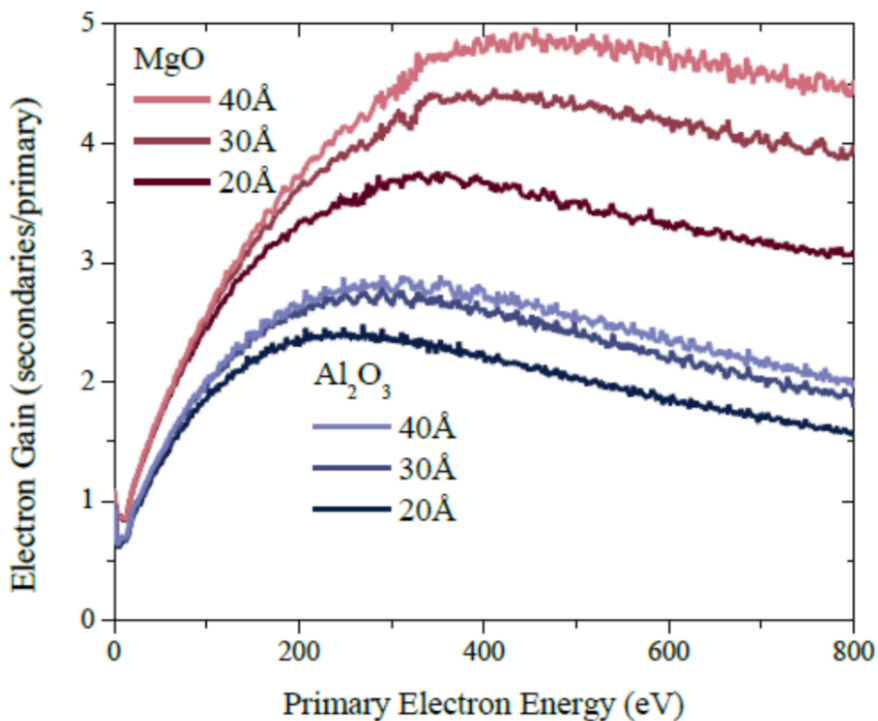


TCR as a function of resistivity – A comparison

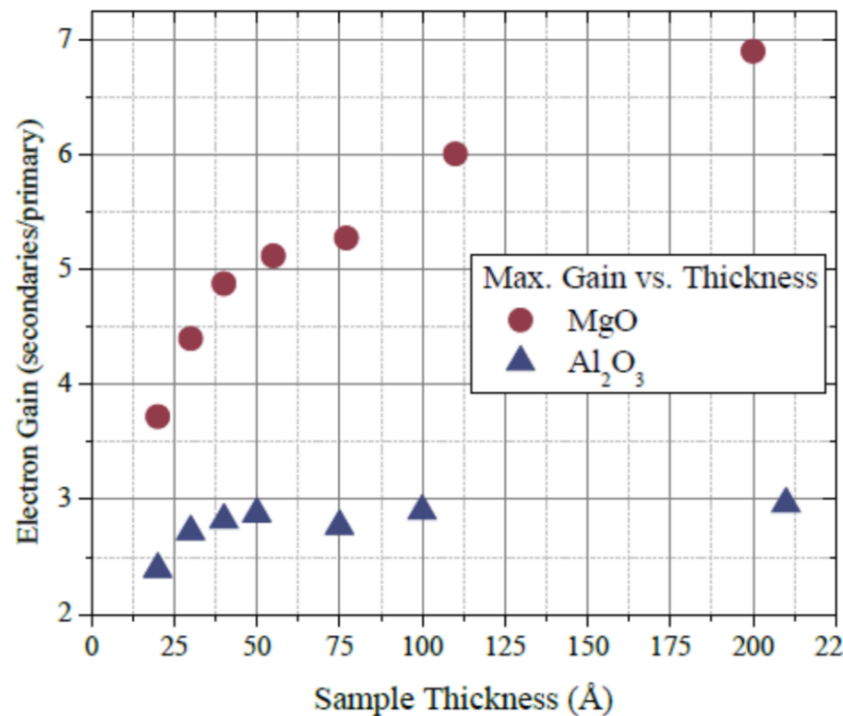
Cross sectional Transmission Electron Microscopy image of ALD $\text{ReAl}_2\text{O}_3\text{CH}_3$ sample grown on Si(100) at 150 °C

X ray diffraction pattern of 70 nm ALD $\text{ReAl}_2\text{O}_3\text{CH}_3$ film prepared at 150 C on Si (100) as deposited (bottom) and after 400 °C anneal (top)

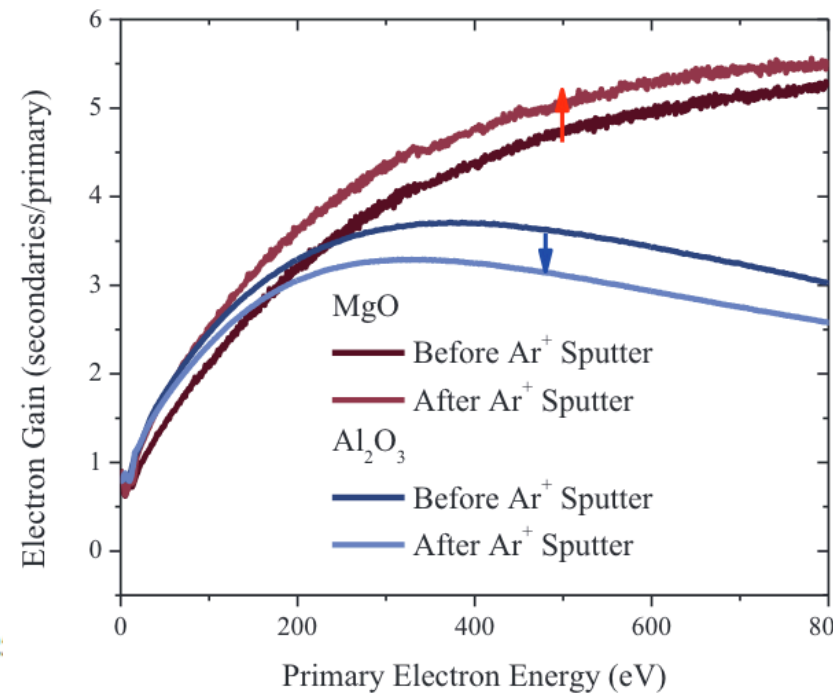
Secondary electron emissive layers for MCP



Electron gain as a function of primary electron energy



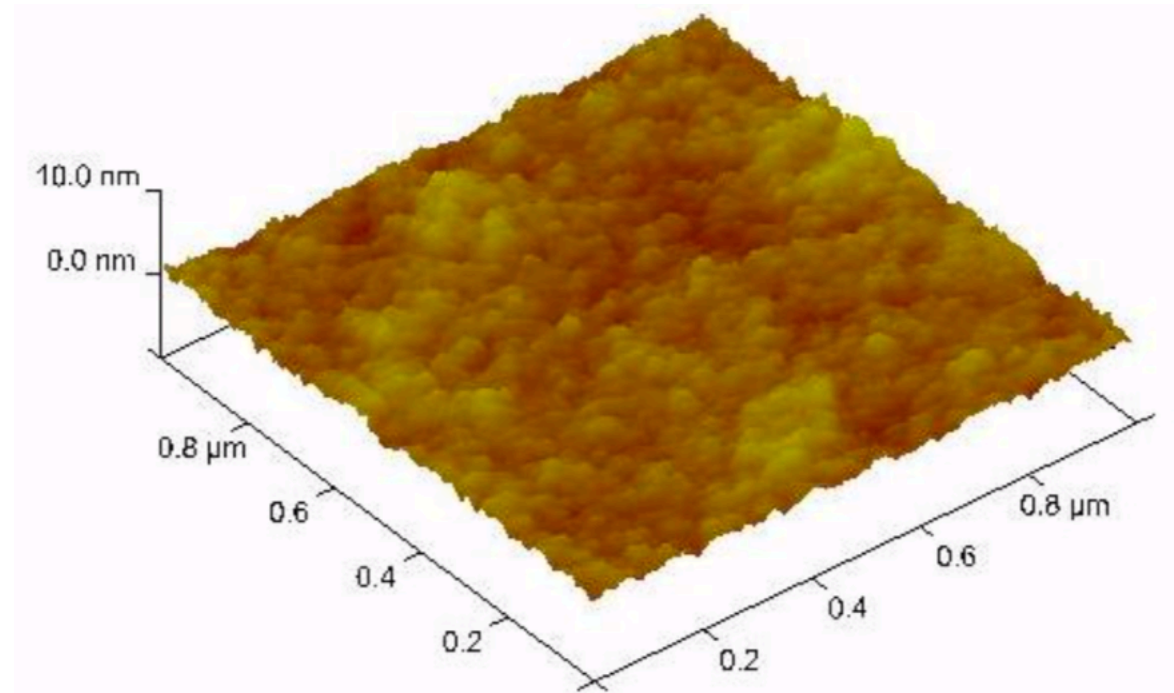
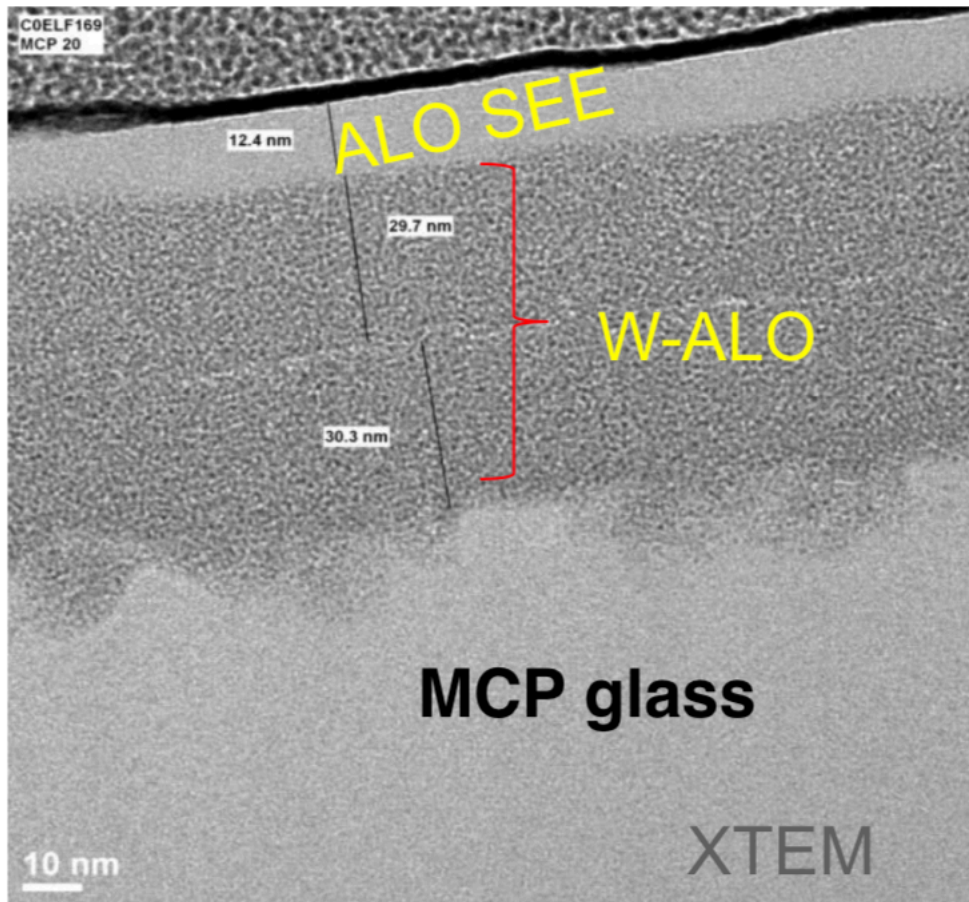
Electron gain as a function of sample thickness



Electron gain as a function of surface composition

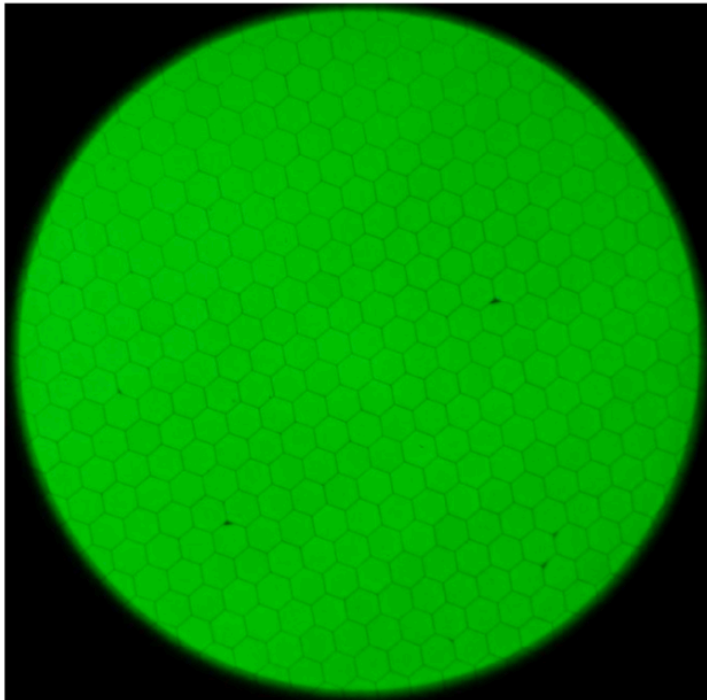
Jokela *et al*, Physics Procedia 37 (2012) 740 – 747

Cross Sectional Microstructure and roughness of ALD WAIFOC resistive layer and Al_2O_3 Secondary electron emissive layer based MCP



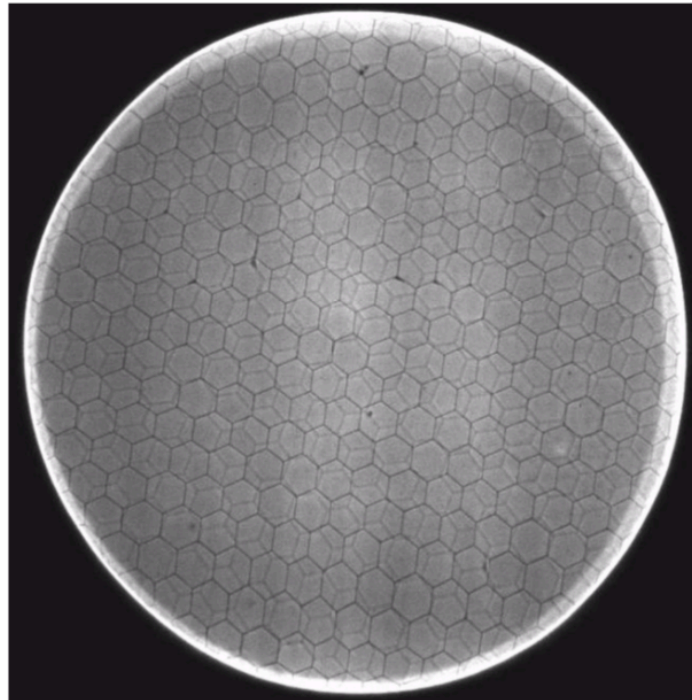
Roughness = 0.6 nm

High Gain MCPs obtained



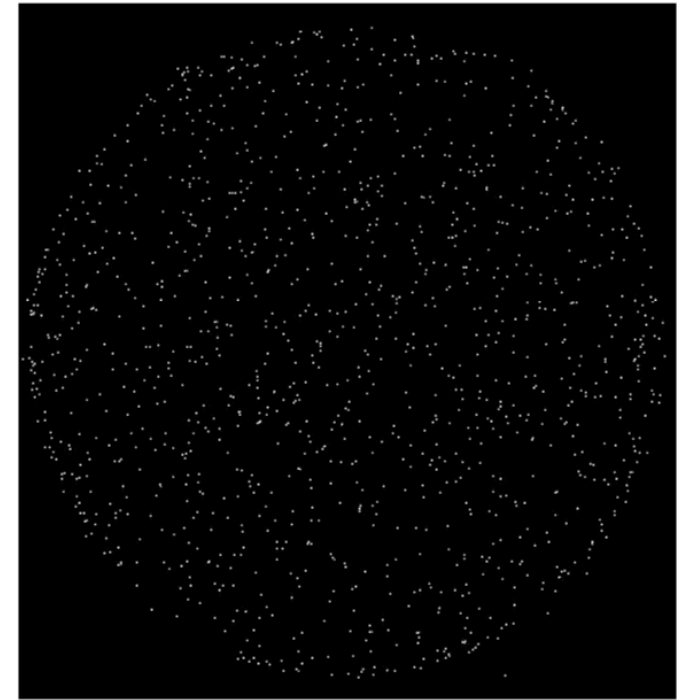
Phosphor image

Single MCP Image (Phosphor)



Gain map

Image of 185nm UV light, **ALD MCP pair, 20 μ m pores, 8 $^\circ$ bias, 60% OAR**, shows top MCP hex modulation and faint MCP hexagonal modulation from bottom MCP

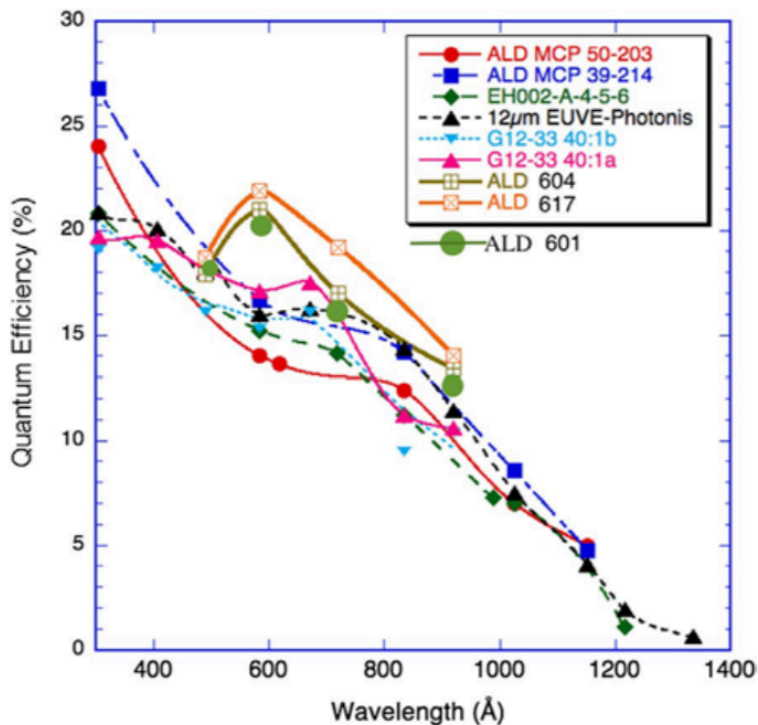


Background counts

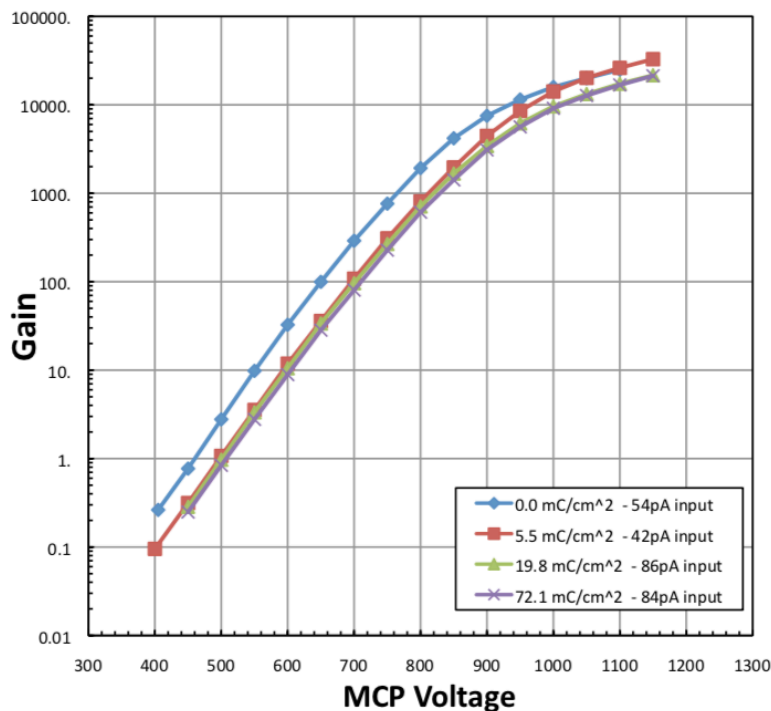
3000 sec background,
0.0845 events/cm²/sec at 7 x 10⁶ gain,
1050v bias each MCP

High gain uniformity and low background

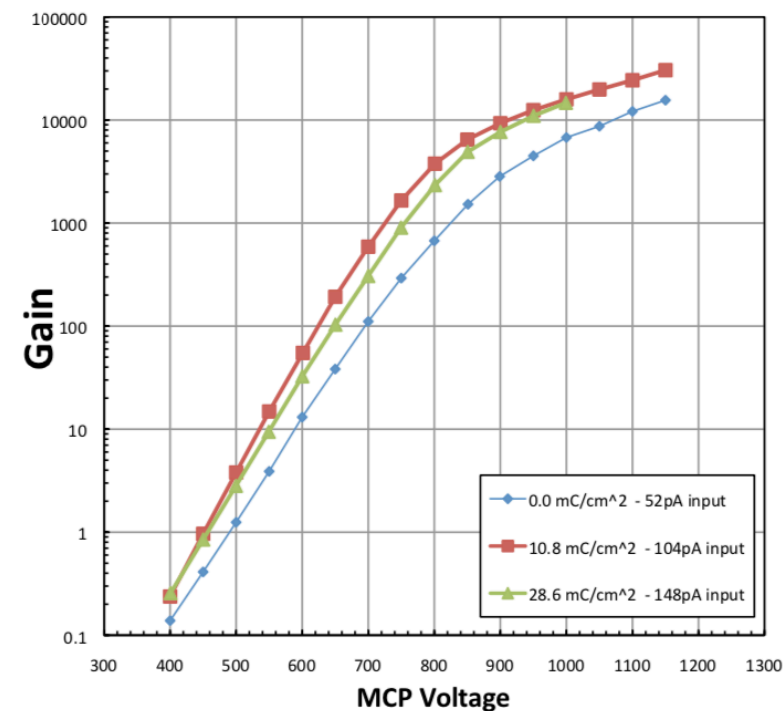
MCP Quantum Efficiency and gain curves



Quantum efficiency of ALD MCPs vs conventional MCPs



Gain characteristics for a 33 mm Al_2O_3 SEE ALD MCP - 20 micron pore, 60:1 L:D during burn in using 200 eV electrons

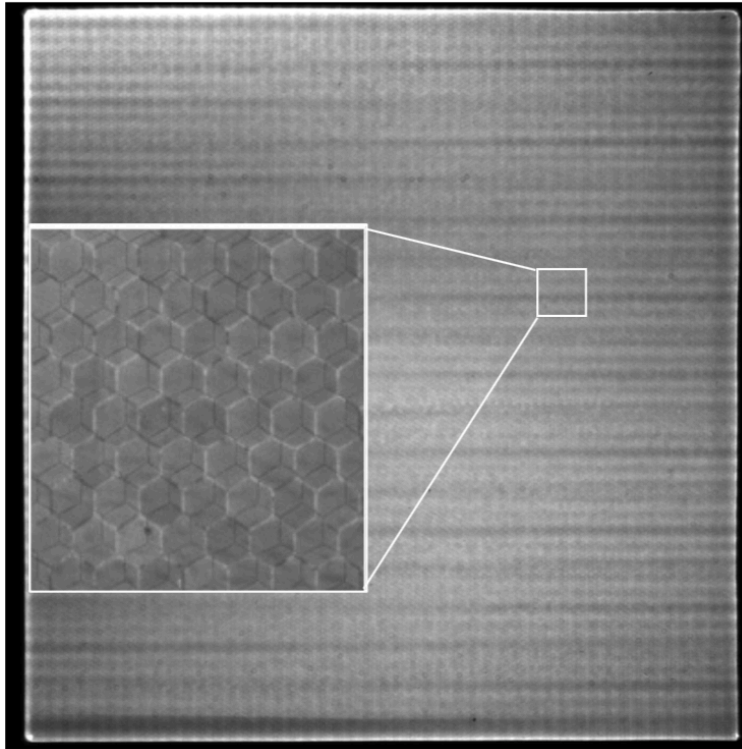


Gain characteristics for a 33 mm MgO SEE ALD MCP - 20 micron pore, 60:1 L:D during burn in using 200 eV electrons

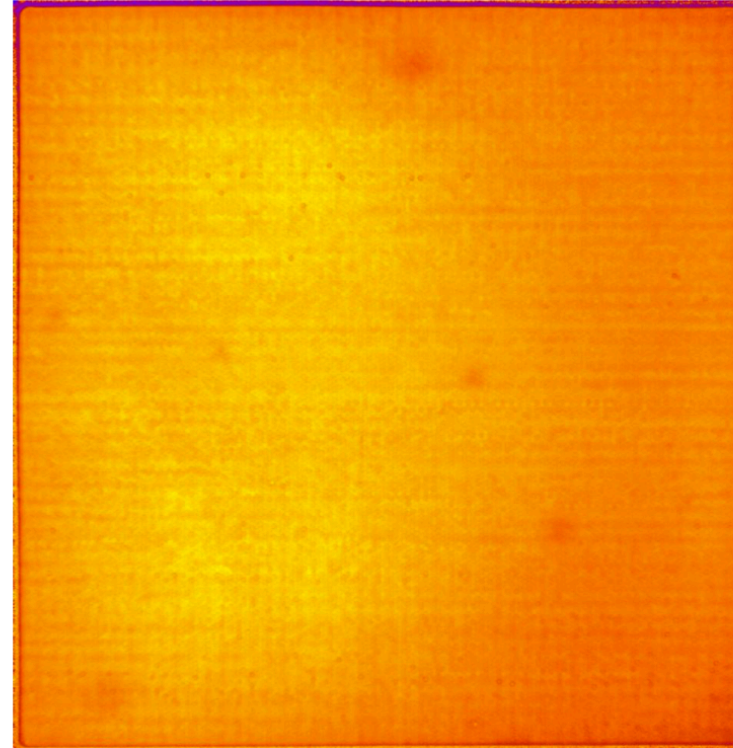
Siegmund et al. – Performance characteristics of atomic layer functionalized microchannel plates PROC SPIE 2013

Large Area MCPs for industry

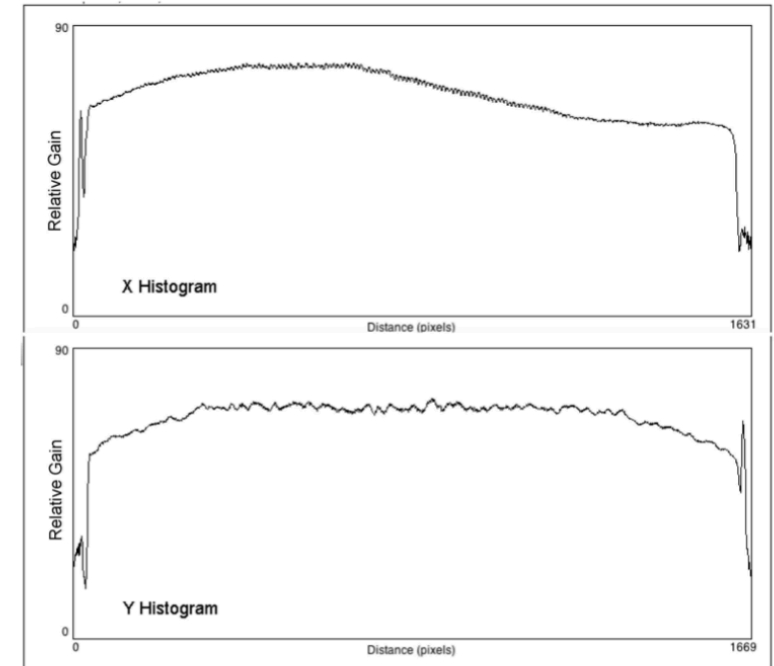
Background counts



Integrated image using 185 nm illumination for a pair of 200 mm square ALD MCPs (20 μ m pore, borosilicate, 60:1 L/d, 8° bias). Inter-MCP 0.7 mm gap with 200v bias.



Integrated gain map using 185 nm illumination for a pair of 200 mm square ALD MCPs (20 μ m pore, borosilicate, 60:1 L/d, 8° bias). Inter-MCP 0.7 mm gap with 200v bias.



Overall gain histograms for the limage on left. Each MCP has a 1000 V bias giving an average gain of 6.5e6. Variations are modest, given the large MCP area.

Siegmund et al. – Performance characteristics of atomic layer functionalized microchannel plates PROC SPIE 2013

Conclusion

1. MCP Operating Principle and Applications Discussed
2. Conventional MCP drawbacks and need for ALD MCPs highlighted
3. ALD MCP resistive and emissive materials, properties and synthesis described
4. High Q.E and gain MCPs fabricated



Acknowledgement

This material is based upon work supported by the Department of Energy/National Nuclear Security Administration under Award Number DE-NA0003921.



ajayaraman@anl.gov

